

This is an Open Access document downloaded from ORCA, Cardiff University's institutional repository:<https://orca.cardiff.ac.uk/id/eprint/75254/>

This is the author's version of a work that was submitted to / accepted for publication.

Citation for final published version:

Finch, Patrick, Hutchings, M. D, Blood, Peter, Sobiesierski, Angela, Smowton, Peter Michael and O'Driscoll, I. D. 2015. Improving the optical bandwidth of passively mode-locked InAs quantum dot lasers. *IEEE Journal of Selected Topics in Quantum Electronics* 21 (6) , 1900507. 10.1109/JSTQE.2015.2416675

Publishers page: <http://dx.doi.org/10.1109/JSTQE.2015.2416675>

Please note:

Changes made as a result of publishing processes such as copy-editing, formatting and page numbers may not be reflected in this version. For the definitive version of this publication, please refer to the published source. You are advised to consult the publisher's version if you wish to cite this paper.

This version is being made available in accordance with publisher policies. See <http://orca.cf.ac.uk/policies.html> for usage policies. Copyright and moral rights for publications made available in ORCA are retained by the copyright holders.



# Improving the Optical Bandwidth of Passively Mode-locked InAs Quantum Dot Lasers

Patrick Finch, Matthew D. Hutchings, Peter Blood, *Fellow, IEEE*, Angela Sobiesierski, *Member, IEEE*, Peter M. Smowton, *Senior Member, IEEE* and Ian O'Driscoll

**Abstract**— We examine in detail the relation between the optical gain spectra, mode-locked optical emission spectra and temporal optical pulsewidths as a function of temperature between 80 K and 300 K on passively mode-locked InAs quantum dot lasers. By increasing the length of the active region, we can decrease the threshold gain requirement for mode-locking. At 300 K, where the dot states and wetting layer are close to thermal equilibrium, the bandwidth of the optical emission spectra and temporal optical pulsewidth remain largely unaffected when the threshold gain requirement is reduced. At 80 K, where the dots are randomly populated, there is a near doubling of the optical bandwidth for the same reduction of the threshold gain requirement and a corresponding decrease in the temporal optical pulsewidth. Rate equations, which take explicit account of the photon density in the cavity, are used to qualitatively highlight the key parameters which are responsible for increasing the optical bandwidth in the random population regime.

**Index Terms** — Quantum Dots, Mode-locking, Semiconductors Lasers, Semiconductor Devices.

## I. INTRODUCTION

It has long been considered important that a wide optical bandwidth is one of the crucial factors in the generation of ultrashort pulses, and for this reason the wide gain spectrum due to inhomogeneous broadening in quantum dot systems has made quantum dots attractive candidates for generation of mode-locked, ultrashort pulses. Thus far, pulsewidths of the order 1 ps and down to 0.4 ps, under optimized conditions of very high drive current and absorber bias, have been achieved with dots at room temperature [1,2] and 0.64 ps pulses from ion-implanted bulk laser diodes [3], compared with 1.3 ps for quantum wells [4] using a two section passively mode-locked device. At room temperature, it is considered and often observed that the dot states are in global thermal equilibrium, following Fermi-Dirac statistics [5], and coupled with each other via the wetting layer. Consequently, the dot occupation is pinned at and above threshold at a value corresponding to the

peak gain, leading to a narrow optical bandwidth and temporally broad optical pulses [6, 7].

When the temperature of the system is brought below approximately 225 K in undoped dots, the occupation becomes nonthermal, and below about 100 K, all ground states across the inhomogeneous distribution have the same occupation probability; this is the random population regime [8]. We have previously shown that the pulsewidths of mode-locked quantum dot devices decrease with decreasing temperature and at 20 K pulsewidths of 300 fs have been achieved using a proton bombarded absorber section [9].

In this paper, we examine in detail the relation between optical gain spectra, mode-locked optical emission spectra and cavity loss, for the same structure as a function of temperature. Using devices of different active region lengths we show that as the width of the accessible gain spectrum is increased by reducing the optical loss, the spectral width of the pulse increases at low temperature, but not at room temperature, thereby accounting for the observed reduction in temporal width of the pulse at low temperature. This interpretation is supported by rate equation modelling of the optical gain spectra above threshold for the inhomogeneous dot distribution. This work confirms that to exploit fully the potential of quantum dots for ultrashort pulse generation, it is necessary to suppress emission of electrons from the dot states to the wetting layer so that each dot behaves as an independent entity.

## I. DEVICE STRUCTURES AND EXPERIMENTAL DETAILS

The samples are comprised of five layers of InAs dots, each grown in a dot-in-a-well (DWELL) on  $\text{In}_{0.15}\text{Ga}_{0.85}\text{As}$  surrounded by a GaAs core and  $\text{Al}_{0.4}\text{Ga}_{0.6}\text{As}$  cladding waveguide. The lengths of the devices were 2 mm and 2.6 mm; with the gain and absorber lengths in the first sample 1.8 mm and 0.2 mm, respectively, and in the second 2.4 mm and 0.2 mm. Each sample consisted of a 50  $\mu\text{m}$  wide oxide stripe with no coating at either facet. The samples were mounted in an Oxford Instruments optical cryostat and cooled using liquid

Manuscript received October, 2014. This research is based on work supported by Science Foundation Ireland (SFI) under Grant No. 11/SIRG/I2131 and Engineering Physical Sciences Research Councils (EPSRC) EP/F006683.

Patrick Finch and Ian O'Driscoll are with CAPPA, Cork Institute of Technology and Tyndall National Institute, Lee Maltings, Cork, Ireland (email:patrick.finch@tyndall.ie; ian.odriscoll@tyndall.ie)

Matthew Hutchings was with School of Physics and Astronomy, Cardiff University, Cardiff CF24 3AA, U. K. He is now with the Physics Department

at Syracuse University, Physics Building, Syracuse, NY, 13244, USA. (email:mdhutc01@syr.edu)

Peter Blood, Angela Sobiesierski and Peter M. Smowton are with the School of Physics and Astronomy, Cardiff University, CF24 3AA, U.K. (email:bloodp@cardiff.ac.uk;kestlea@cardiff.ac.uk; smowtonpm@cardiff.ac.uk)

nitrogen to the desired temperatures, including 300 K, 150 K and 80 K.

In the saturable absorber, the main mechanism by which carriers are lost from the dot at low temperatures is emission to the wetting layer [10] and this becomes very slow below about 225 K [11]. We have therefore bombarded the absorber sections with protons, with energy of 250 keV and dose of  $1 \times 10^{12} \text{ cm}^{-2}$ , to introduce nonradiative recombination centers and increase the recombination rate to reduce the recovery time. This is essential to achieve mode-locking at low temperatures as described in Refs 8 and 10.

Optical spectra were measured using an Ando AQ6317 optical spectrum analyzer, with a resolution of 0.05 nm, and the corresponding autocorrelation traces were obtained using an APE Pulsecheck 150. The mode-locked samples were electrically pulsed with a pulse length of 20  $\mu\text{s}$  and a duty cycle of 8 %.

The modal gain and modal absorption were obtained from single pass measurements of the amplified spontaneous emission [12] using the multi-section technique on 50  $\mu\text{m}$  wide, oxide stripe devices fabricated from the same material with 150  $\mu\text{m}$  section lengths, uncoated facets and pulsed electrical injection.

## II. EXPERIMENTAL RESULTS

Examples of both the optical and gain spectra for various current densities at 300 K are shown in Fig. 1. The optical spectra for the 2 mm device at increments of 110  $\text{A}/\text{cm}^2$ , from 770  $\text{A}/\text{cm}^2$  through to 1100  $\text{A}/\text{cm}^2$  are the upper dotted and dashed lines with peaks centered around 0.947 eV. The optical emission spectra for the 2.6 mm device at the same current densities are the lower dotted and dashed lines with peaks centered around 0.94 eV. The FWHM of the optical spectra for both the 2 mm and 2.6 mm devices are approximately 8 meV.

The optical gain spectra are plotted for increasing currents between 100  $\text{A}/\text{cm}^2$  and 1333  $\text{A}/\text{cm}^2$ . These are measured using non-lasing test structures so any effects of gain pinning that occur in the laser are not seen. The ground state gain peak (0.935 eV-0.95 eV) shifts to higher energies as the level of injection is increased, which we associate with the filling of states in an inhomogeneous distribution [13], and it saturates at higher current densities before shifting back to lower energies due to many body Coulomb interactions [14,15]. Similar behavior is observed for the second peak in the optical gain spectrum, at around 1.02 eV, which we associate with higher lying transition energies.

The threshold gain requirement of a laser is given by

$$G = \frac{L_a}{L_g} A_0 + (\alpha_m + \alpha_i) \frac{L}{L_g} \quad (1)$$

where  $G$  is the modal gain of the active region, length  $L_g$ ,  $A_0$  is the unbombarded band to band modal absorption of the passive absorber section, length,  $L_a$ , and  $\alpha_m$ ,  $\alpha_i$  are the distributed mirror and internal optical losses respectively and  $L$  is the total device length =  $L_a + L_g$  [17]. In our experiments, increasing the length of the gain section lowers the threshold gain requirement

while the other parameters remain fixed. The mirror losses are calculated using  $\alpha_m = \frac{1}{L} \log\left(\frac{1}{\sqrt{R_1 R_2}}\right)$  with  $R_1, R_2 = 0.33$ .  $\alpha_i = 5 \text{ cm}^{-1}$ , is measured from the multi section technique, together with a wavelength dependent absorption  $A_0$ . The thick upper and lower lines in Fig. 1, indicate the calculated threshold gain requirement for mode-locking for the 2 mm and 2.6 mm devices respectively. The intersection of these lines with the gain spectra shows the maximum bandwidth of available gain for each cavity length and this is reduced in the lasing structures when gain / carrier density pinning occurs.

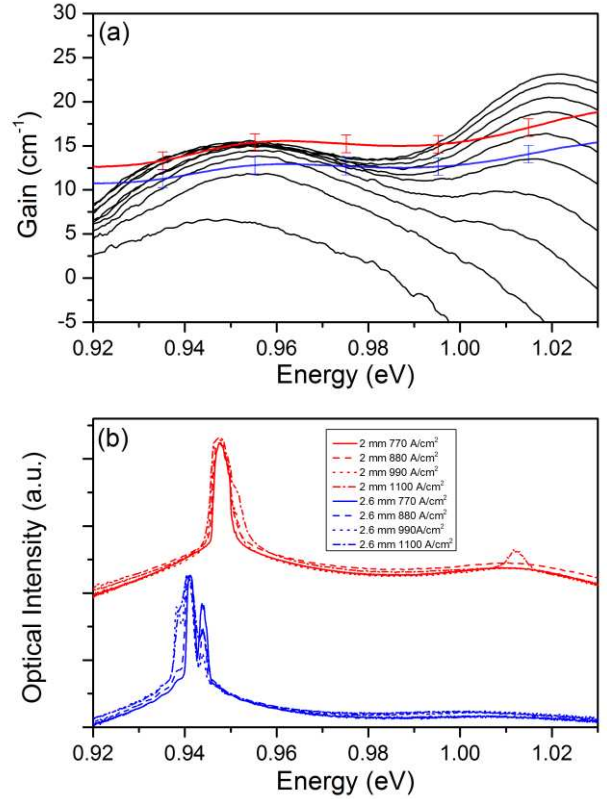


Fig. 1(a): (Color online) 300 K plot of gain vs energy (black lines), with increasing current from 133  $\text{A}/\text{cm}^2$  to 1333  $\text{A}/\text{cm}^2$ , in increments of 133  $\text{A}/\text{cm}^2$ , and threshold gain requirement for 2 mm (red line) and 2.6 mm (blue line) devices.

Fig. 1(b): Corresponding 300 K optical spectra for the 2 mm & 2.6 mm devices, ranging from 770  $\text{A}/\text{cm}^2$  to 1100  $\text{A}/\text{cm}^2$ . There is little difference between the FWHMs of the optical emission spectra as the threshold gain requirement is lowered (red to blue).

Fig. 1 shows that the optical emission spectra shift to higher energies for the short cavity device, as expected from the optical gain spectra. Lowering the threshold gain requirement increases the bandwidth of available gain but this has a marginal effect on the observed bandwidth of the optical emission spectra at room temperature. This is because the dot states and wetting layer are close to thermal equilibrium [8]. At high current density, for the 2 mm device, a second peak is visible in the

optical emission spectra at higher energies, due to the high energy peak in the gain spectra.

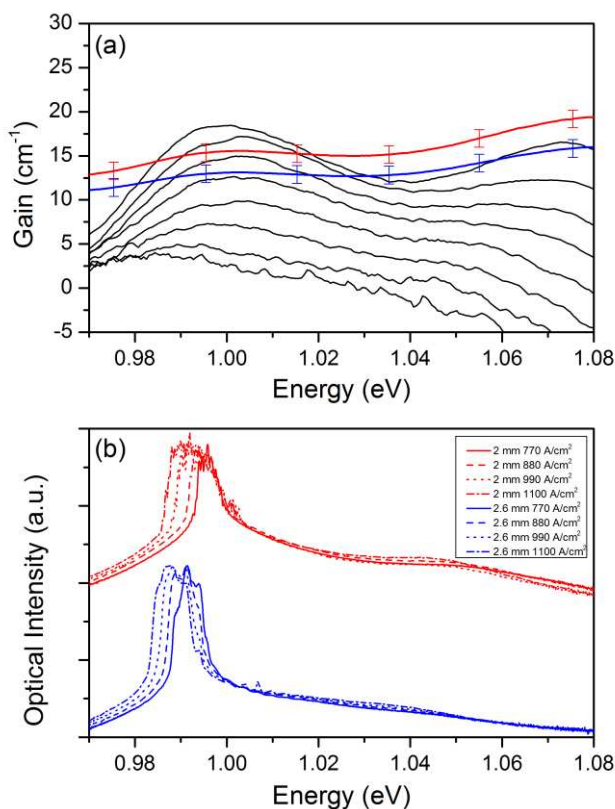


Fig. 2(a): (Color online) 150 K plot of gain vs energy (black lines) for increasing current from 133 A/cm<sup>2</sup> to 1066 A/cm<sup>2</sup>, in 133 A/cm<sup>2</sup> increments, and threshold gain requirement for 2 mm (red line) and 2.6 mm (blue line) devices.

Fig. 2(b): Corresponding 150 K optical spectra for the 2 mm & 2.6 mm devices, ranging from 770 A/cm<sup>2</sup> to 1100 A/cm<sup>2</sup>. More gain is available above each threshold gain requirement compared to 300 K, and the FWHM of the optical emission spectra is marginally increased.

Modal gain and optical emission spectra for the two devices at 150 K are shown in Fig. 2 together with the calculated threshold gain requirements. Compared with 300 K, the peak of the modal gain at the ground state has increased from 15 cm<sup>-1</sup> to 18 cm<sup>-1</sup> for the same level of injection whereas the magnitude of the higher lying peak has been reduced due to the decreased occupancy of the higher lying energy states as the temperature is reduced. The shift of the ground state gain peak to higher energies as the current has increased is also less significant. There is a slight increase in the width of the optical emission spectra as the temperature is reduced and this is mainly due to the reduction in gain saturation and therefore the increased amount of gain available above the threshold gain requirement. Lowering the threshold gain requirement has little effect on the width of the optical emission spectrum. However the optical emission spectra become wider as the current is increased,

which suggests that the carrier density is not fully clamped at this temperature.

Fig. 3 shows optical emission and optical gain spectra and the same threshold gain requirement for the two devices at 80 K. Compared with 300 K, the energy dependence of the gain peak with increasing current is very weak. We suppose this is because the lower energy states are no longer in thermal equilibrium with the wetting layer or with each other and are populated with equal probability independent of their energy. Consequently the gain spectrum follows the inhomogeneous energy distribution of the dot states.

In Fig. 3, the bandwidth of available gain spectra above the threshold gain requirement is much greater than at room temperature for both devices, and embraces the higher energy gain peak. The optical emission spectra also include emission from the higher lying transitions though this is not continuous with the low energy emission. At 80 K, it is clear that the optical emission spectra are wider for the device with the greater active length, which is consistent with the greater bandwidth of available gain. The gain spectra in Fig. 3 are measured using a non-lasing test structure so any effects of gain pinning that occur in the laser are not seen. Without gain pinning the lasing spectral width of the lasing device is determined by the spectral width where the gain exceeds the gain requirement (loss). Our interpretation of the change in ground state emission spectrum is that it broadens on both high and low energy sides because of the reduced gain requirement. The degree of broadening on the low energy side is consistent with the increase spectral width of gain above the gain requirement (loss) level.

At 80 K, the higher peak in the optical emission spectra shifts to lower energies, as the threshold condition is reduced and we hypothesize this is due to the fact that the higher lying energy states (shallower dots) are still able to communicate with the wetting layer and their occupation is not truly random. However, the size of the shift one would expect due to the change in energy where net gain is first obtained in the excited state for each threshold condition appears to be small to completely explain this effect and it may be due to the propagating pulse experiencing a greater degree of amplification and dispersion in the longer gain section. We were not able to observe mode competition effects in our devices.

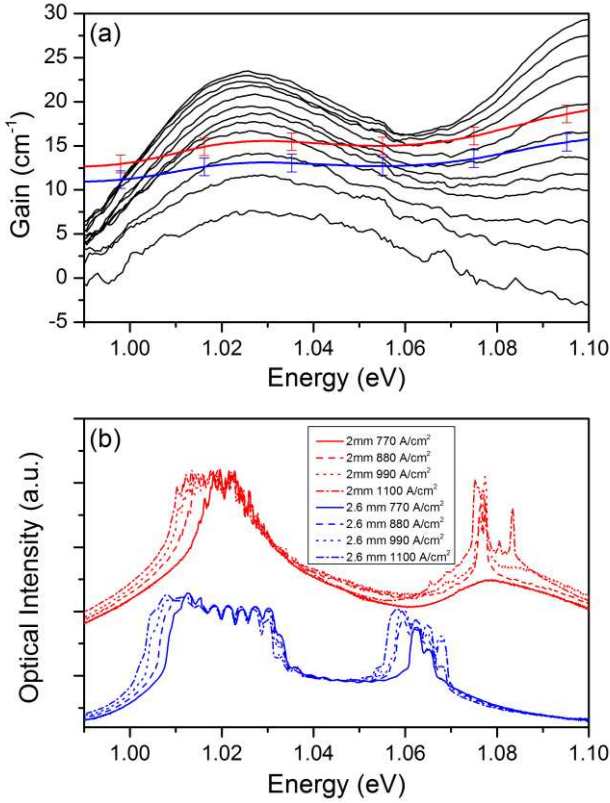


Fig. 3(a): (Color online) 80 K plot of gain vs energy (black lines) for increasing current from 100 A/cm<sup>2</sup> to 800 A/cm<sup>2</sup>, in 66 A/cm<sup>2</sup> increments, and threshold gain requirement for 2 mm (red line) and 2.6 mm (blue line) devices.

Fig. 3(b): Corresponding 80 K optical spectra for the 2 mm & 2.6 mm devices, ranging from 770 A/cm<sup>2</sup> to 1100 A/cm<sup>2</sup>. By lowering the gain threshold condition at 80 K, there is a significant increase in the FWHM of the optical emission spectra.

We observed that the corresponding temporal optical pulsewidths for each set of optical emission spectra decrease significantly at 80 K, across a range of equivalent reverse biases and current densities, consistent with the observed spectral widths. As an example, at 80 K, at a reverse bias of 4 V and current density of 1100 A/cm<sup>2</sup>, the pulsewidth of the shorter device was measured to be 940 fs whereas the longer device was 610 fs, which corresponds to a decrease of more than a third. In general, we observed a 30-40% decrease in the temporal optical pulsewidth across a range of reverse biases as the threshold gain requirement was lowered from the shorter to longer device.

It should be noted that other parameters, apart from the gain section length, in the calculation of the gain threshold condition can be manipulated in order to allow access to even more of the gain spectrum. These include the saturable absorber section length and the internal and mirror losses. Optimizing of the growth conditions in order to lower defects will help lower the internal losses while the mirror losses can be lowered using

high reflectivity coatings which have the added benefit of creating self-colliding pulse effects in the saturable absorber for pulse narrowing [17]. For the purposes of this experimental work, only manipulation of the gain section length was undertaken.

### III. RATE EQUATION ANALYSIS

In order to further understand our experimental data, we have studied the effect of capture, emission and recombination at the dot states on the gain spectrum above threshold by means of a set of carrier, phonon and photon rate equations. These treat the electronic transitions between the wetting layer and ground state of the dots as interactions with a Bose-Einstein distribution of phonons [8]. Previously, these equations were used to compute the behavior at threshold, where the peak gain was set equal to the optical loss, but in order to understand the behavior above threshold we have to take explicit account of the photon density by including a coupled single-mode photon rate equation for the cavity. These rate equations are not an attempt to simulate the actual devices measured in Sec II but rather use a simple model to illustrate qualitatively the link between thermal and non-thermal behavior and the shape of the spectra. For such purposes, we did not go to the considerable added complexity of including a coupled population for the excited states as such a solution is not readily obtained. The energy states are calculated for harmonic potentials in an inhomogeneous Gaussian distribution of 51 transition energies and we assume the dots are occupied by electron hole pairs. The net rate of change of electrons in the ground state of the active region is given by

$$\frac{dn}{dt} = R_{\uparrow} - R_{\downarrow} - R_{spont} - R_{stim} \quad (2)$$

where  $R_{\uparrow}$  and  $R_{\downarrow}$  are the phonon-mediated upward and downward rates of exchange of carriers between the ground states and wetting layer. Carriers on the dots are lost by spontaneous,  $R_{spont}$ , and net stimulated recombination,  $R_{stim}$ . The thermal distribution of phonons at a temperature  $T$  is given by

$$n_{th} = \frac{1}{\exp\left(\frac{h\nu}{k_B T}\right) - 1} \quad (3)$$

and the energy required for an electron to be emitted from a dot to the wetting layer is provided by the absorption of a phonon, while the energy released when an electron is captured to a dot results in the emission of a phonon [18].  $h\nu$  is the energy separation between the dot state and wetting layer. The number of electrons occupying the ground state is  $n = f_g N_d$  for  $N_d$  dots per unit area where  $f_g$  is the ground state occupation probability.

The downward rate,  $R_{\downarrow}$ , from an occupied wetting layer state to an empty localized dot state is given by  $B_0(n_{th} + 1)f_w(1 - f_g)N_d$  where  $B_0$  is a rate constant with units cm<sup>2</sup>s<sup>-1</sup>,  $f_w$  is the wetting layer occupancy, and the first and second components of the term  $(n_{th} + 1)$  account for the stimulated and spontaneous emission of a phonon respectively. The

upward rate,  $R_{\uparrow}$ , from an occupied dot state to an empty wetting layer state, is  $B_0 n_{th} f_g (1 - f_w) N_d$ . The spontaneous emission rate of a photon,  $R_{spont}$ , is given by  $\frac{f_g N_d}{\tau_{spont}}$  where  $\tau_{spont}$  is the spontaneous recombination time with a value of 1 ns. Full details are given in Ref 7.

The carriers are coupled to the photon population through stimulated emission, net rate  $R_{stim}$ , which is equal to  $v_g G N_{ph}$  where  $v_g$  is the group velocity,  $G$  is the modal gain and  $N_{ph}$  is the number of photons per unit area. The single mode rate equation for the cavity in the steady state gives,

$$N_{ph} = \frac{\beta_{spont} R_{spont}}{\frac{1}{\tau_{ph}} - v_g G} \quad (4)$$

where  $\beta_{spont}$  is the fraction of light coupled to the mode and  $\tau_{ph}$  is the cold cavity photon lifetime representing the average rate at which photons are lost from the cavity and is inversely proportional to the total optical loss. The calculation of the modal gain,  $G$ , as a function of  $n$ , incorporates homogenous broadening with a temperature dependent linewidth taken from Ref 19. The calculation does not include bandgap narrowing.

All the calculations were done for a laser without a passive absorber for three different values of optical loss of  $\alpha_i + \alpha_m = 5, 10, 15 \text{ cm}^{-1}$  at each temperature, representing the effect of changing the length of the gain region. These values span the range of optical loss in the experiments. Reverse voltage applied on the absorber is known to impact pulse shape and optical emission spectra. Our calculation assumes that the absorber recovery time is always fast enough and our calculations do not include the intermediate situations where reverse bias can adjust the absorber recovery time.

Fig. 4 (a) shows the Gaussian inhomogeneous dot distribution with a standard deviation and ground state peak chosen to match the measured absorption spectra of the laser structures. Figs 4 (b) and (c) are the calculated ground state occupation probability,  $f_g$ , (by solving equation (2)) and modal gain spectra at 300 K for an optical loss of 5, 10 and 15  $\text{cm}^{-1}$  and a current density of  $1.5 \times J_{th}$  in each case. Threshold in the model was identified, as in an experiment, by extrapolating the light current curve to the current axis.

At 300 K, near threshold, the calculated occupation probability is close to a Fermi-Dirac distribution and the occupation decreases with increasing energy. However we find that, with the rate constants used in the model, the occupation distribution deviates from this at higher current as the stimulated recombination rate increases, as is suggested by experimental observations [20]. This behavior is shown in Fig. 5, for an optical loss of 5  $\text{cm}^{-1}$  and at multiples of threshold current.

As the optical loss is increased, the gain peak shifts to higher energies (Fig. 4(c)) towards the energy peak of the dot distribution (Fig. 4(a)). The peak gain is pinned above threshold and the laser emission at each loss occurs at the peak of the gain spectrum with a narrow linewidth and any current above threshold supplies the lasing process rather than increasing the population of dots across the inhomogeneous distribution.

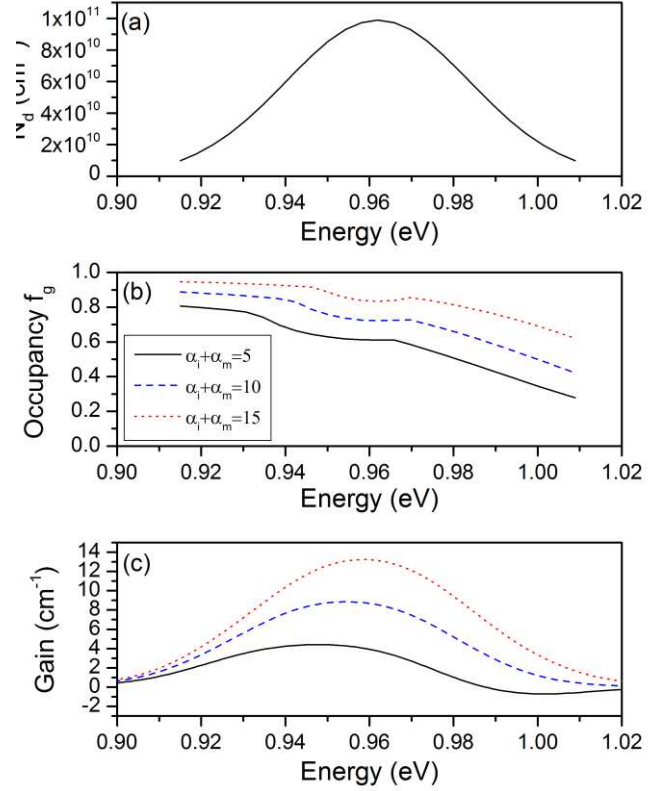


Fig. 4: (Color online) (a) Plot of the number of dots per unit area versus energy (b) 300 K plot of dot occupancy  $f_g$  vs energy at  $1.5 \times J_{th}$  (c) 300 K plot of gain vs energy at  $1.5 \times J_{th}$  for three different optical losses: 5  $\text{cm}^{-1}$  (solid line), 10  $\text{cm}^{-1}$  (dashed line) and 15  $\text{cm}^{-1}$  (dotted line). Lasing occurs only at the peak of the gain spectrum for all cases resulting in a narrow optical spectrum.

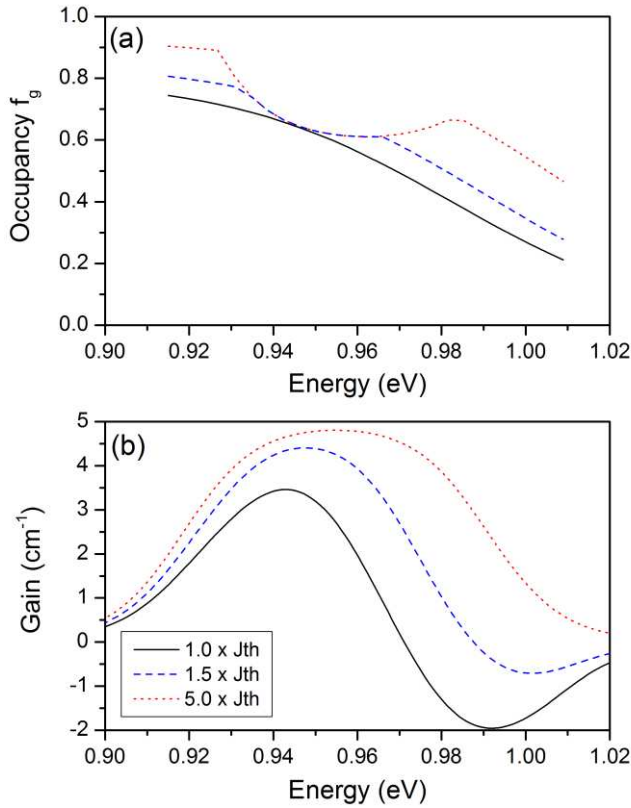


Fig. 5: (Color online) (a) 300 K plot of dot occupancy  $f_g$  versus energy (b) modal gain vs energy for an optical loss of  $5 \text{ cm}^{-1}$  at multiples of the threshold current  $J_{th}$ . Increasing  $f_w$  corresponds to an increase in the current. Increasing injection causes little change in the width of the peak of the gain spectrum.

At 80 K,  $f_g$  was calculated for the same three values of optical loss and is plotted as a function of energy in Fig. 6(a) together with the corresponding optical gain in Fig. 6(b) for the same energy distribution of dot states in Fig. 4(a) whereas the ground state peak energy was shifted in accordance with the experimentally measured modal absorption spectra at 80 K. We find that at 80 K, the ground state dots are populated randomly and below threshold the occupation probability is the same for all the ground states, so the gain spectrum follows the dot state distribution (Fig. 4(a)) and laser action is initiated at the peak of this distribution with a narrow line. At threshold current, the gain of those dots which contribute to laser action is clamped at the cavity loss (Fig. 6(b)) and their occupation increases with energy away from the peak (Fig. 6(a) to compensate for decreasing dot density (Fig. 4(a)). As the optical loss is lowered, more dots are inverted and the spectrum broadens compared to 300 K for the same loss in Fig. 4(c).

In Fig. 7, we have plotted  $f_g$  and optical gain as a function of energy for a fixed loss of  $5 \text{ cm}^{-1}$  at multiples of the threshold current density  $J_{th}$  determined by choice of the wetting layer occupation. It can be seen that the occupancy of the dots which do not contribute to lasing increases with increasing current

until their gain matches the optical loss. Those carriers are supplied from the same wetting layer and since the recombination at these dots is due only to spontaneous emission, their

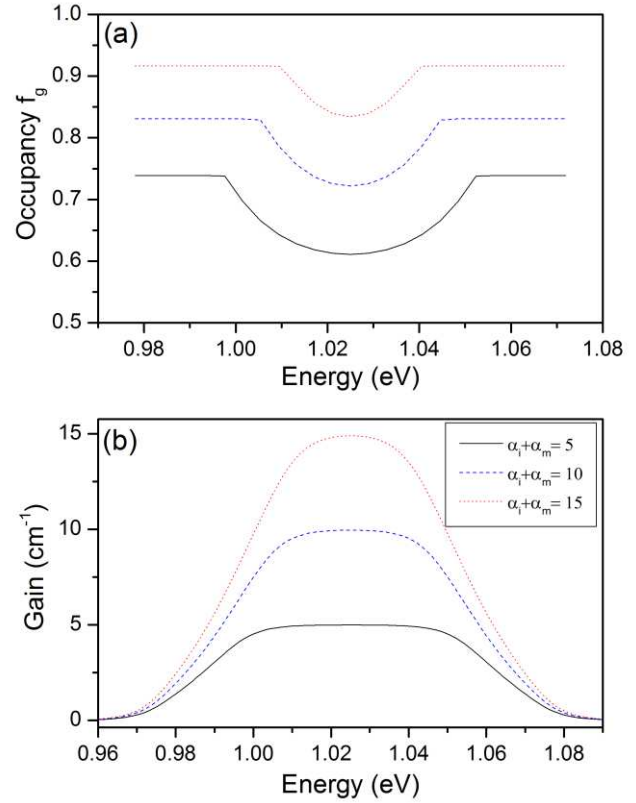


Fig. 6: (Color online) (a) 80 K plot of dot occupancy  $f_g$  vs energy (b) modal gain vs energy at  $1.5 \times J_{th}$  for three different optical losses:  $5 \text{ cm}^{-1}$  (solid line),  $10 \text{ cm}^{-1}$  (dashed line) and  $15 \text{ cm}^{-1}$  (dotted line). By lowering the threshold gain requirement the gain spectrum is broadened as more and more dots are accessible.

occupancy rises with increasing wetting layer carrier density,  $f_w$ . For the dots which contribute to laser action, their occupation is the inverse of the dot distribution and their occupation does not change once lasing is initiated. Gradually the non-lasing dots contribute to lasing as their occupation increases with increasing injection as  $f_w$  is increased. Thus, more of the carriers that are required to invert more dots are provided by the external current and not the depletion of other dots. Therefore, the optical spectrum broadens as more and more dots become inverted. This behavior is in contrast to the model at 300 K as shown in Fig. 5, for the same optical loss and same multiples of threshold current density where the gain spectrum remains narrow and almost unchanged for increasing injection. The pinning of the gain spectra, observed in Figs 6 and 7 at 80 K, is not observed for the gain spectra in Fig 3 at 80 K as these spectra are measured in non-lasing test structures using the multi section technique [12]. At 80 K, the

calculated escape rates from the dots to the wetting layer becomes very slow so the model no longer predicts a Fermi-Dirac distribution [9].

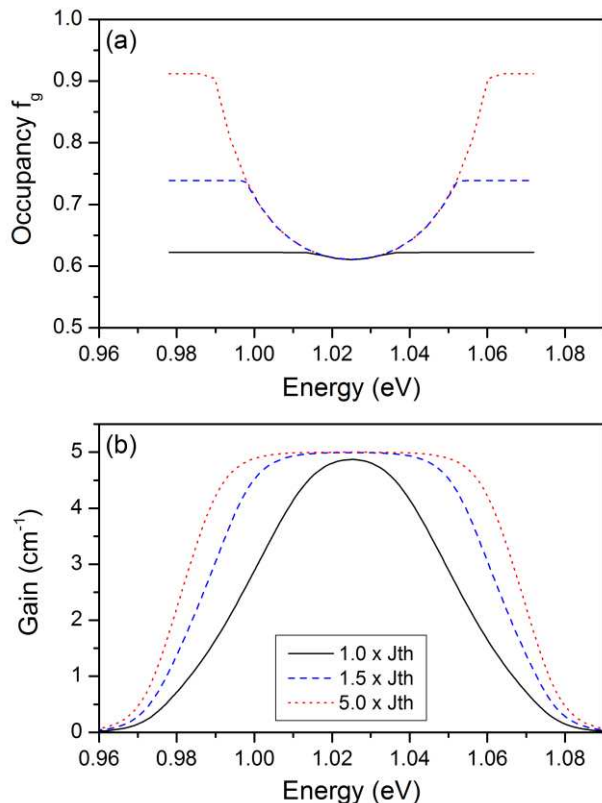


Fig. 7: (Color online) (a) 80 K plot of dot occupancy  $f_g$  versus energy (b) modal gain vs energy for an optical loss of  $5 \text{ cm}^{-1}$  at multiples of the threshold current  $J_{th}$ . Increasing  $f_w$  corresponds to an increase in the current. The occupancy  $f_g$  is clamped above threshold, whereas the gain spectrum broadens with increasing current as more dots contribute to lasing.

The calculations show that at room temperature where the dots are close to thermal equilibrium with the wetting layer the width of the gain spectrum does not change above threshold, nor does it depend upon cavity length. The emission occurs at the gain peak irrespective of the bandwidth of the gain available above the optical loss.

At low temperature, in the random population regime, the width of the gain spectrum increases with current and with decreasing optical loss. This is consistent with the measured emission spectra in Fig. 3 and confirms that in this regime the spectral width of the optical emission increases with increasing bandwidth of the gain available above the threshold gain requirement.

#### IV. CONCLUSIONS

We have studied the influence of the cavity loss on the duration of optical pulses produced by passive mode locking of InAs quantum dot lasers as a function of temperature. At room temperature and at low temperature, in the random population regime, we compare the optical gain and laser emission spectra, pulse duration and solve a set of single-mode rate equations for the coupled carrier, photon and phonon populations. At room temperature, the cavity loss has no discernible effect on the spectral width and duration of the optical pulses whereas at 80 K we measure an increase in spectral width and reduction in pulsewidth from typically 940 fs to 610 fs when the cavity loss is reduced by from 14 to  $11 \text{ cm}^{-1}$ , a modest reduction of only 20 %. Rate equations show that in the random population regime a reduction in cavity loss results in an increase in the width of the gain spectrum at and above threshold because the populations in different size dots are no longer coupled by carrier emission to the wetting layer. This work confirms the merits of random population of quantum dots for generation of ultra-short pulses and shows that the pulsewidth can be reduced by the relatively simple method of reducing the optical cavity loss.

#### ACKNOWLEDGMENTS

We would like to thank R. M. Gwilliam at the University of Surrey, U. K. for the proton bombardment.

- [1] E. U. Rafailov, M. A. Cataluna, W. Sibbett, N. D. Il'inskaya, Yu. M. Zadiranov, A. E. Zhukov, V. M. Ustinov, D. D. Livshits, A. R. Kovsh and N. N. Ledentsov, "High-power picosecond and femtosecond pulse generation from a two-section model-locked quantum dot laser", *Appl. Phys. Lett.* 87, 081107, August 2005.
- [2] Mark G. Thompson, Alastair R. Rae, Mo Xia, Richard V. Penty, and Ian H. White, "InGaAs Quantum-Dot Mode-Locked Laser Diodes", *IEEE J. Sel. Topics in Quantum Electron.*, vol. 15, No. 3, May/June 2009.
- [3] A. G. Deryagin, D. V. Kuksenkov, V. I. Kuchinskii, E. L. Portnoi, I. Yu. Khrushchev, J. Frahm, "Generation of high repetition subpicosecond pulses at  $1.535 \mu\text{m}$  by passive mode-locking of InGaAs/InP laser diode with saturable absorber regions created by ion implantation", *14<sup>th</sup> IEEE ISLC*, 107-108, Sep. 1994.
- [4] Dennis J. Derickson, Roger J. Helkey, Alan Mar, Judy R. Karin, John G. Wasserbauer and John E. Bowers, "Short Pulse Generation Using Multisegment Mode-Locked Semiconductor Laser", *IEEE J. Quantum Elec.*, vol. 28, no. 10, October 1992.
- [5] H. D. Summers, J. D. Thomson, P. M. Snowton, P. Blood, and M. Hopkinson, "Thermodynamic balance in quantum dot lasers", *Semi-cond. Sci. Technol.*, vol. 16, p. 140, Nov. 2001.
- [6] E. U. Rafailov, M. A. Cataluna, and W. Sibbett, "Mode-locked quantum-dot lasers", *Nat. Photon.*, vol. 1, pp. 395-401, 2007.
- [7] M. Kuntz, G. Fiol, M. Laemmlin, C. Meuer, and D. Bimberg, "High-Speed Mode-Locked Quantum-Dot Lasers and Optical Amplifiers", *Proc. IEEE*, vol. 95, no. 9,

- pp. 1767–1778, Sep. 2007.
- [8] I. O’Driscoll, Peter Blood, and Peter M. Smowton, “Random Population of Quantum Dots in InAs–GaAs Laser Structures”, *IEEE J. Quantum Elec.*, 46, 4, June 2010.
- [9] P. Finch, P. Blood, P. M. Smowton, A. Sobiesierski, R. M. Gwilliam and I. O’Driscoll, “Femtosecond pulse generation in passively mode-locked InAs quantum dot lasers”, *Appl. Phys. Lett.* 103, 131109, Sep. 2013.
- [10] G. Gelinas, A. Lanacer, R. Leonelli, R. A. Masut, and P. J. Poole, “Carrier thermal escape in families of InAs/InP self-assembled quantum dots”, *Phys.Rev. B*, 81, 235426, June 2010.
- [11] O’Driscoll, P. Blood, P. M. Smowton, A. Sobiesierski, and R. Gwilliam, “Effect of proton bombardment on InAs dots and wetting layer in laser structures”, *Appl. Phys. Lett.*, 100, 261105, Oct. 2012.
- [12] P. Blood, G. M. Lewis, P. M. Smowton, H. D. Summers, J. D. Thomson, and J. Lutti, “Characterization of semiconductor laser gain media by the segmented contact method,” *IEEE J. Sel. Topics Quantum Electron.*, vol. 9, no. 5, pp. 1275–1281, Sep./Oct.2003.
- [13] M. Hutchings, I. O’Driscoll, P. M. Smowton and P. Blood, “Temperature dependence of the gain peak in p-doped InAs quantum dot lasers”, *Appl. Phys. Lett.*, 99, 151118, Oct 2011.
- [14] I. O’Driscoll, M. Hutchings, P. M. Smowton and P. Blood, “Many-body effects in InAs-GaAs laser structures”, *Appl. Phys. Lett.* 97, 141102, Oct. 2010.
- [15] H. C. Schneider and W. W. Chow, “Many-body effects in the gain spectra of highly excited quantum-dot lasers”, *Phys. Rev. B*, 64, 115315, August 2001.
- [16] C. Y. Lin, Y. C. Xin, Y. Li, F. L. Chiragh and L. F. Lester, “Cavity design and characteristics of monolithic long-wavelength InAs/InP quantum dash passively mode-locked lasers”, *Optics Express*, 19740, Vol. 17, No. 22, Oct. 2009.
- [17] M. Crowley, D. Murrell, N. Patel, M. Breivik, C. Y. Lin, Y. Li, B-O. Fimland, L. Lester, “Analytical Modeling of the Temperature Performance of the Monolithic Passively Mode-Locked Quantum Dot Lasers”, *IEEE J. Quantum Electron.*, vol. 47, no. 8, Aug. 2011.
- [18] H. Huang and D. G. Deppe, “Rate equation model for non equilibrium operating conditions in a self organized quantum dot laser,” *IEEE J. Quantum Electron.*, vol. 37, no. 5, pp. 691–698, May 2001.
- [19] P. Borri, W. Langbein, S. Schneider, U. Woggon, R. L. Sellin, D. Ouyang, and D. Bimberg, “Exciton relaxation and dephasing in quantum dot amplifiers from room to cryogenic temperature,” *IEEE J. Sel. Topics Quantum Electron.*, vol. 8, no. 5, pp. 984–991, Sep./Oct. 2002.
- [20] Igor P. Marko, Alf R. Adams, Nicolas F. Massé, Stephen J. Sweeney, “Effect of non-pinned carrier density above threshold in InAs quantum dot and quantum dash lasers”, *IET Optoelectronics*, vol. 8, pp88-93, April 2014.